AIAA JOURNAL
Vol. 43, No. 11, November 2005

Minimum-State Unsteady Aerodynamics for Aeroservoelastic Configuration Shape Optimization of Flight Vehicles

Marat Mor* and Eli Livne†
University of Washington, Seattle, Washington 98195-2400

The minimum-state technique for creating linear-time-invariant state-space models of unsteady aerodynamic loads leads to major savings in terms of the dimension of the resulting aeroservoelastic systems compared to alternative techniques. The up-front effort of the generation of minimum-state approximants, however, is large and involves an iterative double least-squares function fitting process. When the overall shape of a configuration varies during the repetitive analysis required for configuration design optimization, the cost of creating new minimum-state approximations becomes prohibitive. This paper presents an efficient method for obtaining shape sensitivity analysis of minimum-state approximants. The resulting sensitivities are then used, based on a single detailed analysis and sensitivity analysis at some reference design to generate approximate aeroelastic poles, divergence speed, and flutter speed results for configurations that are subject to considerable planform shape changes.

Nomenclature

$[A]$	=	state-space model aeroelastic matrix
$[A_0], [A_1], [A_2], \ldots$	=	rational approximation matrices
b	=	reference semichord length of wing
$[C]$	=	damping matrix
c	=	chord length of wing
$[D], [E]$	=	rational approximation matrices of lag terms
DV	=	design variable
E	=	Young modulus
G	=	shear modulus
$[I]$	=	identity matrix
j	=	pure imaginary number, $-\sqrt{1}$
$[K]$	=	stiffness matrix
k	=	reduced frequency
L	=	half-span length of wing
$\{L_{\text{vec}}\}, \{R_{\text{vec}}\}$	=	left and right eigenvectors
$[M]$	=	mass matrix
n	=	number of states
n_k	=	number of reduced frequencies
n_{lag}	=	number of lag terms
p	=	nondimensional Laplace variable
$[Q]$	=	aerodynamic generalized force coefficients matrix
$[\bar{Q}]$	=	approximated aerodynamic generalized force coefficients matrix
q_D	=	dynamic pressure
$[R]$	=	diagonal matrix of lag roots
$[S]$	=	diagonal matrix of singular values
s	=	Laplace variable
$s_{11}, s_{22}, s_{33}, \ldots$	=	singular values
t	=	width of wing
$[U], [V]$	=	singular vectors
V	=	speed of flight
$\{x\}$	=	state vector [Eq. (13)]
$\{x_{\text{lag}}\}$	=	vector of aerodynamic states [Eq. (16)]
γ	=	roots of lag terms
ε	=	accumulated absolute error [Eq. (30)]
Λ_i	=	inboard sweep angle of wing
ξ	=	vector of generalized structural dynamic motions
ρ	=	density
ω	=	frequency of oscillation

Subscripts and Superscripts

D	=	divergence
F	=	flutter
REF	=	reference point
$*$	=	conjugate

Received 11 April 2004; presented as Paper 2004-1762 at the AIAA/ASME/ASCE/AHS/ASC Structures, Structural Dynamics, and Materials Conference, Palm Springs, CA, 19–22 April 2004; revision received 20 January 2005; accepted for publication 19 March 2005.

*Postdoctoral Research Fellow, Department of Aeronautics and Astronautics.

†Professor, Department of Aeronautics and Astronautics. Associate Fellow AIAA.

I. Introduction

DESIGN-ORIENTED unsteady aerodynamic analysis tools for aeroservoelastic shape optimization lag significantly behind other multidisciplinary design optimization (MDO) developments for aerospace vehicle design. In almost all MDO studies to date involving configuration shape optimization, dynamic aeroelastic/aeroservoelastic constraints had to be left out. Flutter, gust stresses, vibration, fatigue, ride comfort, handling qualities, and other control/structure/aerodynamic interactions—all extremely important—still cannot be accounted for efficiently in an automated design process involving configuration shape variations. The reason is that efficient general design-oriented technology for producing unsteady aerodynamic loads and their state-space models for aeroelastic/aeroservoelastic shape design of general configurations is still in its infancy, leading to a gap in every current flight vehicle MDO capability.[1]

Linear unsteady generalized aerodynamic forces are usually computed for simple harmonic motions to yield complex matrices $[Q(jk_l)]$ evaluated at a tabulated set of reduced frequencies $k_l, l = 1, 2, 3, \ldots, n_k$. To create state-space models, a rational function approximation in terms of the reduced frequency k is created by matching a rational function of predetermined structure and order to the tabulated set $[Q(jk_l)]$ in some best way.

When, in the general case, mode shapes used to approximate structural dynamic motion and the configuration shape of the vehicle are subject to change (together with the aerodynamic paneling used), the generalized aerodynamic matrices vary too, depending on shape design variables DV_i. For the subsonic case using a kernel-function solution approach and for both the subsonic and supersonic cases using panel methods, analytic sensitivities $\partial[Q(jk)]/\partial DV$ of

generalized force matrices with respect to planform shape design variables had been derived for planar lifting surface configurations.[2–6] First steps in the development of general configuration shape sensitivities of linear unsteady aerodynamics for the three-dimensional flight vehicle case, including any combination of bodies and lifting surfaces, have recently been reported.[7]

Assuming that shape sensitivities of unsteady aerodynamic load matrices $\partial[Q(jk)]/\partial DV$ are available from capabilities such as Refs. 2–7, it is the goal of this paper to present shape sensitivity techniques for the rational function approximation matching part of the aeroelastic/aeroservoelastic shape optimization modeling problem. Aeroelastic and aeroservoelastic state-space models make it possible to use the powerful techniques of modern control for aeroservoelastic analysis and design. The development of shape sensitivities discussed here is expected to lead to better integration of modern control and aeroelasticity for efficient structures/aerodynamics/controls design synthesis early in the flight-vehicle design process.

II. Aeroelastic State-Space Equations of Motion and Their Sensitivities

The linear aeroelastic problem (without gust excitation and control system) can be formulated in the Laplace domain as follows[1,8]:

$$\left\{s^2[M]+s[C]+[K]-q_D[Q(s)]\right\}\{\xi(s)\}=0 \tag{1}$$

where $[Q(s)]$ is the Laplace-transformed aerodynamic generalized force coefficients matrix. The vector of generalized structural dynamic motions using some modal base is $\{\xi(s)\}$. To create a linear-time-invariant (LTI) state-space model of the system, an approximation of the $[Q]$ matrix in the form of a rational function is introduced:

$$[Q(p)]\approx[A_0]+p[A_1]+p^2[A_2]+p[D]([I]p-[R])^{-1}[E] \tag{2}$$

$$p=s(b/V) \tag{3}$$

The rational function representation of Eq. (2) for the aerodynamic generalized force matrix is convenient because it captures both the Roger[9] and minimum-state (MIST[10–14]) methods.

Linear unsteady aerodynamic loads are usually calculated for simple harmonic motion. They depend on Mach number and the reduced frequency of oscillation:

$$k=\omega b/V \tag{4}$$

With the $\approx$ sign denoting a rational right-hand side approximating the actual transcendental dependency of $[Q(jk)]$ on k, Eq. (2) leads to

$$[Q(jk)]\approx[A_0]+jk[A_1]+(jk)^2[A_2]+jk[D](jk[I]-[R])^{-1}[E] \tag{5}$$

In the case of the Roger approximation,

$$[Q(jk)]\approx[A_0]+jk[A_1]+(jk)^2[A_2]+[jk/(jk+\gamma_1)][A_3]+[jk/(jk+\gamma_2)][A_4]+\cdots \tag{6}$$

Or, written in the form of Eq. (5),

$$[Q(jk)]\approx[A_0]+jk[A_1]+(jk)^2[A_2]+jk[[A_3][A_4]\cdots]\times\begin{bmatrix}(jk+\gamma_1)[I] & [0] & \cdots\\ [0] & (jk+\gamma_2)[I] & \cdots\\ \cdots & \cdots & \cdots\end{bmatrix}^{-1}\begin{bmatrix}[I]\\ [I]\\ \cdots\end{bmatrix} \tag{7}$$

In the minimum-state (MIST) approximation

$$[Q(jk)]\approx[A_0]+jk[A_1]+(jk)^2[A_2]+jk[D]\times\begin{bmatrix}(jk+\gamma_1) & 0 & \cdots\\ 0 & (jk+\gamma_2) & \cdots\\ \cdots & \cdots & \cdots\end{bmatrix}^{-1}[E] \tag{8}$$

In the most common application of both methods, the matrices

$$[R]_{\text{MIST}}=-\begin{bmatrix}\gamma_1 & 0 & \cdots\\ 0 & \gamma_2 & \cdots\\ \cdots & \cdots & \cdots\end{bmatrix} \tag{9}$$

$$[R]_{\text{Roger}}=-\begin{bmatrix}\gamma_1[I] & [0] & \cdots\\ [0] & \gamma_2[I] & \cdots\\ \cdots & \cdots & \cdots\end{bmatrix} \tag{10}$$

are selected a priori to be a diagonal with positive entries on the diagonal to prevent spurious aerodynamic instabilities in the approximation [Eq. (2)].

Substituting Eqs. (2) and (3) into Eq. (1), one obtains a new approximate system of equations:

$$\left\{s^2[\bar{M}]+s[\bar{C}]+[\bar{K}]-s\cdot q_D[D]([I]s-(V/b)[R])^{-1}[E]\right\}\{\xi(s)\}=0 \tag{11}$$

Here

$$[\bar{M}]=[M]-q_D(b/V)^2[A_2],\qquad [\bar{C}]=[C]-q_D(b/V)[A_1]$$

$$[\bar{K}]=[K]-q_D[A_0] \tag{12}$$

Definition of a new state vector in the time domain

$$\{x\}^T=\{\xi\quad\dot{\xi}\quad x_{\text{lag}}\} \tag{13}$$

now yields the state-space open-loop free aeroelastic system of equations of motion:

$$\{\dot{x}\}=[A]\{x\} \tag{14}$$

where the system's matrix is

$$[A]=\begin{bmatrix}[0] & [I] & [0]\\ -[\bar{M}]^{-1}[\bar{K}] & -[\bar{M}]^{-1}[\bar{C}] & q_D[\bar{M}]^{-1}[D]\\ [0] & [E] & (V/b)[R]\end{bmatrix} \tag{15}$$

A vector of aerodynamic states (Laplace transformed)

$$\{x_{\text{lag}}(s)\}=s([I]s-(V/b)[R])^{-1}[E]\{\xi(s)\} \tag{16}$$

has been introduced. Its dimension varies between n_{lag} for the MIST method and $n_{\text{lag}}\times n$ for Roger, where n is the number of generalized coordinates. The minimum-state approximation leads to LTI state-space models that are much smaller in order than corresponding models created using Roger approximations. With a structural dynamic model using, for example, $n=40$ generalized coordinates, and with four lag terms in the Roger case, the dimension of the resulting state-space model is $(2+n_{\text{lag}})n=240$. With 10 aerodynamic lag terms in a minimum-state model, the dimension of the resulting state-space model is $2n+n_{\text{lag}}=90$ only.

Sensitivity of the aeroelastic LTI system matrix with respect to some design variable DV should be found by differentiating Eq. (15):

$$\left[\frac{\partial A}{\partial DV}\right]=\begin{bmatrix}0 & 0 & 0\\ -\dfrac{\partial([\bar{M}]^{-1}[\bar{K}])}{\partial DV} & -\dfrac{\partial([\bar{M}]^{-1}[\bar{C}])}{\partial DV} & q_D\dfrac{\partial([\bar{M}]^{-1}[D])}{\partial DV}\\ 0 & \left[\dfrac{\partial E}{\partial DV}\right] & 0\end{bmatrix} \tag{17}$$

The derivatives of the matrices $[\bar{M}]$, $[\bar{C}]$, and $[\bar{K}]$ are obtained as follows:

$$\left[\frac{\partial\bar{M}}{\partial DV}\right]=\left[\frac{\partial M}{\partial DV}\right]-q_D\frac{b^2}{V^2}\left[\frac{\partial A_2}{\partial DV}\right] \tag{18}$$

$$\left[\frac{\partial \bar{C}}{\partial DV}\right] = \left[\frac{\partial C}{\partial DV}\right] - q_D \frac{b}{V}\left[\frac{\partial A_1}{\partial DV}\right] \tag{19}$$

$$\left[\frac{\partial \bar{K}}{\partial DV}\right] = \left[\frac{\partial K}{\partial DV}\right] - q_D\left[\frac{\partial A_0}{\partial DV}\right] \tag{20}$$

A number of techniques are currently available for calculating sensitivities of structural finite element matrices with respect to either sizing-type or shape design variables, and this technology is already implemented in a number of commercial finite element codes.[15,16] The focus of the work reported here is on the sensitivities of the aerodynamic rational function approximation matrices. Sensitivity analysis of Roger rational function approximation matrices $[A_0], [A_1], [A_2], \ldots$ and the corresponding aeroservoelastic poles had been reported in Refs. 4–6. The problem of sensitivity analysis in the case of the minimum-state approximation is more complex, and a brief review of MIST model generation process is required before the major issues can be addressed.

A. Iterative Generation of MIST Approximants

Starting with

$$[Q(k)] \approx [A_0] + jk[A_1] - k^2[A_2] + [D]\begin{bmatrix} \dfrac{k}{k - j\gamma_1} & 0 & 0 \\ 0 & \dfrac{k}{k - j\gamma_2} & 0 \\ 0 & 0 & \ddots \end{bmatrix}[E] \tag{21}$$

we can separate real and imaginary parts because

$$\frac{k}{k - j\gamma_i} = \frac{k^2 + jk\gamma_i}{k^2 + \gamma_i^2} \tag{22}$$

Thus,

$$Re[Q(k)] \approx [A_0] - k^2[A_2] + [D]\begin{bmatrix} \dfrac{k^2}{k^2 + \gamma_1^2} & 0 & 0 \\ 0 & \dfrac{k^2}{k^2 + \gamma_2^2} & 0 \\ 0 & 0 & \ddots \end{bmatrix}[E] \tag{23}$$

$$\mathrm{Im}[Q(k)] \approx k[A_1] + [D]\begin{bmatrix} \dfrac{k\gamma_1}{k^2 + \gamma_1^2} & 0 & 0 \\ 0 & \dfrac{k\gamma_2}{k^2 + \gamma_2^2} & 0 \\ 0 & 0 & \ddots \end{bmatrix}[E] \tag{24}$$

The goal is to obtain an accurate approximation that will fit tabulated data throughout the frequency range. Using the tabulated data obtained at a set of tabulated reduced frequencies $k_l, l = 1, 2, 3, \ldots, n_k$ Eq. (23) together with Eq. (24) lead to the following system of $2n_k$ approximation conditions:

$$\begin{cases} -k_l^2[A_2] + [D][\Pi_R(k_l)][E] \\ \quad \approx \mathrm{Re}[Q(k_l)] - [A_0] \\ k_l[A_1] + [D][\Pi_I(k_l)][E] \\ \quad \approx \mathrm{Im}[Q(k_l)] \end{cases}, \qquad l = 1, 2, 3, \ldots, n_k \tag{25}$$

where the diagonal matrices $[\Pi_R(k_l)]$ and $[\Pi_I(k_l)]$ (which are functions of tabulated reduced frequencies k_l) are defined as follows:

$$[\Pi_R(k_l)] = \begin{bmatrix} \dfrac{k_l^2}{k_l^2 + \gamma_1^2} & 0 & 0 \\ 0 & \dfrac{k_l^2}{k_l^2 + \gamma_2^2} & 0 \\ 0 & 0 & \ddots \end{bmatrix} \tag{26}$$

$$[\Pi_I(k_l)] = \begin{bmatrix} \dfrac{k_l\gamma_1}{k_l^2 + \gamma_1^2} & 0 & 0 \\ 0 & \dfrac{k_l\gamma_2}{k_l^2 + \gamma_2^2} & 0 \\ 0 & 0 & \ddots \end{bmatrix} \tag{27}$$

The matrix $[A_0]$ is set to equal the steady $[Q(jk = 0)]$. The search for the MIST matrices is then carried out in an iterative manner. An initial value $[D_0]$ is assigned to the $[D]$ matrix. A linear least-squares problem can now be solved for elements of $[A_1]$, $[A_2]$, and $[E]$ as follows.

The matrix form of the system of the preceding equations [Eq. (25)] is

$$\begin{bmatrix} [0] & -k_1^2[I] & [D][\Pi_R(k_1)] \\ k_1[I] & [0] & [D][\Pi_I(k_1)] \\ [0] & -k_2^2[I] & [D][\Pi_R(k_2)] \\ k_2[I] & [0] & [D][\Pi_I(k_2)] \\ \cdots & \cdots & \cdots \\ [0] & -k_{n_k}^2[I] & [D]\left[\Pi_R\left(k_{n_k}\right)\right] \\ k_{n_k}[I] & [0] & [D]\left[\Pi_I\left(k_{n_k}\right)\right] \end{bmatrix}\begin{bmatrix} [A_1] \\ [A_2] \\ [A_3] \end{bmatrix} \approx \begin{bmatrix} \mathrm{Re}[Q(k_1)] - [A_0] \\ \mathrm{Im}[Q(k_1)] \\ \mathrm{Re}[Q(k_2)] - [A_0] \\ \mathrm{Im}[Q(k_2)] \\ \cdots \\ \mathrm{Re}\left[Q\left(k_{n_k}\right)\right] - [A_0] \\ \mathrm{Im}\left[Q\left(k_{n_k}\right)\right] \end{bmatrix} \tag{28}$$

Premultiplication of the left- and right-hand sides by the matrix

$$\begin{bmatrix} [0] & -k_1^2[I] & [D][\Pi_R(k_1)] \\ k_1[I] & [0] & [D][\Pi_I(k_1)] \\ [0] & -k_2^2[I] & [D][\Pi_R(k_2)] \\ k_2[I] & [0] & [D][\Pi_I(k_2)] \\ \cdots & \cdots & \cdots \\ [0] & -k_{n_k}^2[I] & [D]\left[\Pi_R\left(k_{n_k}\right)\right] \\ k_{n_k}[I] & [0] & [D]\left[\Pi_I\left(k_{n_k}\right)\right] \end{bmatrix}^T$$

leads to a minimum least-squares approximation solution for the matrices $[A_1]$, $[A_2]$, and $[E]$ assuming a given matrix $[D]$.

Next, fixing the elements of the $[E]$ matrix to those found from the least-squares solution just described, we now formulate a least-squares problem for elements of a new $[D]$ matrix as follows.

Similar to the preceding process, the matrix form of the system presented in Eq. (25) for the matrix variables $[A_1]$, $[A_2]$, and $[D]$ is

$$\begin{bmatrix} [A_1] & [A_2] & [D] \end{bmatrix}\begin{bmatrix} [0] & k_1[I] & \cdots & [0] & k_{n_k}[I] \\ -k_1^2[I] & 0 & \cdots & -k_{n_k}^2[I] & 0 \\ [\Pi_R(k_1)][E] & [\Pi_I(k_1)][E] & \cdots & \left[\Pi_R\left(k_{n_k}\right)\right][E] & \left[\Pi_I\left(k_{n_k}\right)\right][E] \end{bmatrix}$$

$$\approx \begin{bmatrix} \mathrm{Re}[Q(k_1)] - [A_0] & \mathrm{Im}[Q(k_1)] & \cdots & \mathrm{Re}\left[Q\left(k_{n_k}\right)\right] - [A_0] & \mathrm{Im}\left[Q\left(k_{n_k}\right)\right] \end{bmatrix} \tag{29}$$

Postmultiplication by the system's coefficient matrix leads to a second least-squares problem for the matrices $[A_1]$, $[A_2]$, and $[D]$. The iterative process now continues with the fixing of the new $[D]$ and searching for new $[A_1]$, $[A_2]$, and $[E]$ [Eq. (28)], etc. Note that the solution for the matrices $[D]$, $[E]$ is not unique, and it depends on the initial guess for the $[D]$ matrix, which starts the iteration process.

The procedure just outlined is one of possible similar procedures for different variants of the minimum-state method. Other cases include constraints used in order to force the approximated aeroloads to match the tabulated loads (real and/or imaginary parts) at some reduced frequency of importance; thus making it possible to eliminate the matrices $[A_1]$, $[A_2]$. These become completely dependent on $[D]$, $[E]$ in such cases.[13] In another variation of the minimum-state method, different weights are introduced into the least-squares process to achieve better overall accuracy of the match for elements of the $[Q(jk)]$ matrix, which are found to influence more heavily the actual aeroelastic behavior.[12]

The order reduction gains of the MIST method come at a price. The generation of MIST models can be lengthy and, since the introduction of the method, has been done in an iterative process.

B. Convergence

The nonlinear nature of the double least-squares iterative MIST process leads to complicated behavior and convergence issues. In general, for a small number of lags convergence of such a process can be determined based on the accuracy of the matching between the MIST rational function approximant and the tabulated generalized force data. Matching errors have to be considered for all terms of the matrix at all tabulated reduced frequencies. An accumulated absolute error measure is often used:

$$\varepsilon = \left\{ \sum_{i,j=1}^{n} \sum_{m=1}^{n_k} \left[\mathrm{Re}|\bar{Q}_{ij}(k_m) - Q_{ij}(k_m)|^2 \right] + \sum_{i,j=1}^{n} \sum_{m=1}^{n_k} \left[\mathrm{Im}|\bar{Q}_{ij}(k_m) - Q_{ij}(k_m)|^2 \right] \right\}^{\frac{1}{2}} \tag{30}$$

Here $[\bar{Q}]$ is the approximated aerodynamic generalized force coefficients matrix:

$$[\bar{Q}(jk)] = [A_0] + jk[A_1] + (jk)^2[A_2] + jk[D](jk[I] - [R])^{-1}[E] \tag{31}$$

The iterative MIST process stops when the difference between the matching errors in two consequent iterations reaches below a certain threshold.

The rise in cost, because of the need to repetitively carry out aeroelastic simulations, can be significant, though. Physical weights, introduced into the double least-squares matching process and accounting for relative importance of different terms based on open-loop response of the reference structure, provide a more economical way computationally for taking overall aeroelastic behavior into account during the matching process. In the case of design optimization, however, the reference design used for the creation of MIST approximants can end up quite different in mass and stiffness distributions from systems evolving from it. The value of physical weights that were determined at the reference design point might be questionable.

Although the stopping criteria just mentioned work well for a relatively small number of lags (usually $n_{\mathrm{lag}} < 5$, depending on the number of states), it is costly and sometimes impossible to implement them in cases when the number of lags is becoming large. The number of iterations can reach thousands and tens of thousands (depending on a case) before the stopping criteria will terminate the process. Moreover, even if a change in the matching errors [Eq. (30)] in two consequent iterations satisfies the criteria, the change in the matrices $[D]$ and $[E]$ can be very significant. This is a result of the nonlinear nature of the problem as well as the nonuniqueness of the solution for the matrices $[D]$ and $[E]$. It is clear that any multiplication of one of these matrices by any number and corresponding division of the other matrix by the same number would still lead to the same approximation results. As a matter of fact, depending on the starting point for the matrix $[D]$ the evolution of the $[D]$ and $[E]$ matrices during the iterative matching process can exhibit jumps and branch changes. Fortunately, the change in the solution's branch usually does not have significant influence on the product $[D]$ $[E]$ (which remains almost constant). This fact allows users to terminate the iterative process after 10–20 iterations only even for the problems with a large number of lags without considerably degrading the accuracy of the match.

The iterative nature of the data matching process and its characteristics in the MIST approach are the source of difficulty when sensitivities of this approximation are sought.[17] To better understand it, one needs to reexamine the aerodynamic matrix approximation presented in Eq. (2).

Differentiating this equation with respect to a design variable leads to

$$\left[\frac{\partial Q(p)}{\partial DV}\right] \approx \left[\frac{\partial A_0}{\partial DV}\right] + p\left[\frac{\partial A_1}{\partial DV}\right] + p^2\left[\frac{\partial A_2}{\partial DV}\right] + p\left[\frac{\partial D}{\partial DV}\right] \times ([I]p - [R])^{-1}[E] + p[D]([I]p - [R])^{-1}\left[\frac{\partial E}{\partial DV}\right] \tag{32}$$

The derivative of the static aerodynamic stiffness matrix is calculated using the aerodynamic matrix $[Q]$ at steady state:

$$\left[\frac{\partial A_0}{\partial DV}\right] = \left[\frac{\partial Q(p=0)}{\partial DV}\right] \tag{33}$$

Equation (32) is a linear equation for $[\partial A_1/\partial DV]$, $[\partial A_2/\partial DV]$, $[\partial D/\partial DV]$, $[\partial E/\partial DV]$ and can be solved in a double least-squares manner using the tabulated $[\partial Q(jk_1)/\partial DV]$, $[\partial Q(jk_2)/\partial DV]$, $\ldots$ $[\partial Q(jk_{n_k})/\partial DV]$ But although this approach is reliable in the case of MIST evaluation for $[A_1]$, $[A_2]$, $[D]$, $[E]$ it is questionable when applied to the process of finding derivatives. The sensitivity of MIST matrices to starting guesses and the jumps between solution branches might lead to sensitivities that will not capture (via Taylor-series extrapolations) the matrices $[D]$ and $[E]$ at a new design point DV. In addition, to reduce the calculation time an additional iterative process should be avoided, if possible. This raises the question whether there is any case in which MIST approximations of unsteady aerodynamic loads can be found without the iterative MIST process. Such a case can be used for studying alternative approaches to MIST matrix sensitivity computation. As we show in the following section, it is possible to obtain a MIST approximant without the iterative process in the case of unsteady aerodynamic loads represented by a one-lag Roger approximation.

C. Roger Approximation with One Aerodynamic Lag Term and MIST Without Nonlinear Iterations

When one lag term is used in a Roger approximation of generalized unsteady loads, the aerodynamic force coefficients matrix is approximated by

$$[Q(p)] \approx [A_0] + [A_1]p + [A_2]p^2 + [p/(p+\gamma_1)][A_3] \tag{34}$$

As shown in Refs. 4–6, no iteration is required for obtaining the Roger approximation matrices and their sensitivities. The Roger rational function matching process leads to equations that are linear in the unknown matrices and their sensitivities and involves solutions of simple least-squares problems.

Using the singular value decomposition, the matrix $[A_3]$ can be presented as

$$[A_3] = [U][S][V] = \sum_{i=1}^{n} \{U_i\} s_{ii} \{V_i\}^T \tag{35}$$

where $\{U_i\}$ and $\{V_i\}$ are the singular vectors and $[S]$ is the diagonal matrix of singular values s_{ii}. It can be proven (see Appendix) in

the case of one Roger lag term γ_1 that using the first left and right singular vectors and the associated singular value of the $[A_3]$ matrix (when $[A_3]$ was generated by the Roger approximation) leads to the product $\{D\}\{E\}^T$ of one lag term MIST approximation with the same lag root. That is

$$\{D\}\{E\}^T = \{U_1\}s_{11}\{V_1\}^T \tag{36}$$

Furthermore, if the first m singular values and vectors of $[A_3]$ are taken, the resulting rational function approximation is the same as a MIST approximation generated (starting with the proper $[D]$) with the same number of identical aerodynamic roots γ_1. For example, if we approximate the matrix $[A_3]$ using a three-term singular value decomposition (SVD) series

$$[A_3] = \{U_1\}s_{11}\{V_1\}^T + \{U_2\}s_{22}\{V_2\}^T + \{U_3\}s_{33}\{V_3\}^T \tag{37}$$

then a SVD approximation of the Roger series becomes

$$\begin{aligned}[Q(p)] &= [A_0] + [A_1]p + [A_2]p^2 + \frac{p}{p+\gamma_1}\Big[\{U_1\}s_{11}\{V_1\}^T \\ &\quad + \{U_2\}s_{22}\{V_2\}^T + \{U_3\}s_{33}\{V_3\}^T\Big] \\ &= [A_0] + [A_1]p + [A_2]p^2 \\ &\quad + p[D]\begin{bmatrix} p+\gamma_1 & 0 & 0 \\ 0 & p+\gamma_1 & 0 \\ 0 & 0 & p+\gamma_1 \end{bmatrix}^{-1}[E]\end{aligned} \tag{38}$$

with

$$[D] = [\{U_1\} \quad \{U_2\} \quad \{U_3\}], \qquad [E] = \begin{bmatrix} s_{11}\{V_1\}^T \\ s_{22}\{V_2\}^T \\ s_{33}\{V_3\}^T \end{bmatrix} \tag{39}$$

A Roger approximation using one lag term, then, leads to corresponding $[D]$, $[E]$ matrices by SVD, and those lead to a lag term in a MIST approximation (obtained by an iterative process) that is identical. Once the SVD is used to approximate the $[A_3]$ matrix from the Roger approximation, the corresponding $[D]$, $[E]$ are frozen, and another Roger-like least-squares process is carried out to correct the matrices $[A_1]$, $[A_2]$. Again, no iteration is involved, and the resulting series $[A_0] + p[A_1] + p^2[A_2] + p[D]([I]p - [R])^{-1}[E]$ leads to the same approximant that would have been obtained by the iterative MIST process, when applied with identical roots.

If SVD is used to obtain the MIST lag terms from a Roger approximation, then the derivatives of the lag terms can be written as follows:

$$\frac{\partial\{U_i\}s_{ii}\{V_i\}^T}{\partial DV} = \frac{\partial\{U_i\}}{\partial DV}s_{ii}\{V_i\}^T + \{U_i\}\frac{\partial s_{ii}}{\partial DV}\{V_i\}^T + \{U_i\}s_{ii}\frac{\partial\{V_i\}^T}{\partial DV} \tag{40}$$

With the sensitivity analysis singular values and singular vectors readily available, similar to sensitivity analysis of eigenvalues and eigenvectors (see also Ref. 18), sensitivities of the MIST lag terms can now be found as

$$\begin{aligned} p\frac{\partial[\{U_1\} \quad \{U_2\} \quad \{U_3\}]}{\partial DV}&\begin{bmatrix} p+\gamma_1 & 0 & 0 \\ 0 & p+\gamma_1 & 0 \\ 0 & 0 & p+\gamma_1 \end{bmatrix}^{-1} \\ &\times \begin{bmatrix} s_{11}\{V_1\}^T \\ s_{22}\{V_2\}^T \\ s_{33}\{V_3\}^T \end{bmatrix} + p[\{U_1\} \quad \{U_2\} \quad \{U_3\}] \\ &\times \begin{bmatrix} p+\gamma_1 & 0 & 0 \\ 0 & p+\gamma_1 & 0 \\ 0 & 0 & p+\gamma_1 \end{bmatrix}^{-1} \frac{\partial}{\partial DV}\begin{bmatrix} s_{11}\{V_1\}^T \\ s_{22}\{V_2\}^T \\ s_{33}\{V_3\}^T \end{bmatrix}\end{aligned} \tag{41}$$

and sensitivities of $[\partial A_1/\partial DV]$, $[\partial A_2/\partial DV]$ by least-squares matching

$$\begin{aligned} jk_l\left[\frac{\partial A_1}{\partial DV}\right] + (jk_l)^2\left[\frac{\partial A_2}{\partial DV}\right] &\approx \left[\frac{\partial Q(jk_l)}{\partial DV}\right] - \left[\frac{\partial A_0}{\partial DV}\right] \\ &- jk_l\frac{\partial}{\partial DV}[\{U_1\} \quad \{U_2\} \quad \{U_3\}] \\ &\times \begin{bmatrix} jk_l+\gamma_1 & 0 & 0 \\ 0 & jk_l+\gamma_1 & 0 \\ 0 & 0 & jk_l+\gamma_1 \end{bmatrix}^{-1} \begin{bmatrix} s_{11}\{V_1\}^T \\ s_{22}\{V_2\}^T \\ s_{33}\{V_3\}^T \end{bmatrix} \\ &- jk_l[\{U_1\} \quad \{U_2\} \quad \{U_3\}] \\ &\times \begin{bmatrix} jk_l+\gamma_1 & 0 & 0 \\ 0 & jk_l+\gamma_1 & 0 \\ 0 & 0 & jk_l+\gamma_1 \end{bmatrix}^{-1} \frac{\partial}{\partial DV}\begin{bmatrix} s_{11}\{V_1\}^T \\ s_{22}\{V_2\}^T \\ s_{33}\{V_3\}^T \end{bmatrix}\end{aligned} \tag{42}$$

It can be suggested, however, that similar to a fixed-modes approach in structural dynamics, approximate sensitivities of the SVD terms should be generated by neglecting $\partial\{U\}/\partial DV$, $\partial\{V\}/\partial DV$ terms and keeping only $\partial s_{ii}/\partial DV$ terms. Further examination of Eqs. (32) and (42) shows that the calculation of MIST approximation sensitivities is greatly simplified by neglecting only $\partial\{U\}/\partial DV$ [Eq. (42)] or, equivalently, neglecting only $\partial\{D\}/\partial DV$ [Eq. (32)].

Thus, the following sensitivity expression is to be examined:

$$\begin{aligned}\left[\frac{\partial Q(p)}{\partial DV}\right] &\approx \left[\frac{\partial A_0}{\partial DV}\right] + p\left[\frac{\partial A_1}{\partial DV}\right] + p^2\left[\frac{\partial A_2}{\partial DV}\right] \\ &\quad + p[\{U_1\} \quad \{U_2\} \quad \{U_3\}]\begin{bmatrix} p+\gamma_1 & 0 & 0 \\ 0 & p+\gamma_1 & 0 \\ 0 & 0 & p+\gamma_1 \end{bmatrix}^{-1} \\ &\quad \times \frac{\partial}{\partial DV}\begin{bmatrix} s_{11}\{V_1\}^T \\ s_{22}\{V_2\}^T \\ s_{33}\{V_3\}^T \end{bmatrix}\end{aligned} \tag{43}$$

or, equivalently,

$$\begin{aligned}\left[\frac{\partial Q(p)}{\partial DV}\right] &\approx \left[\frac{\partial A_0}{\partial DV}\right] + p\left[\frac{\partial A_1}{\partial DV}\right] + p^2\left[\frac{\partial A_2}{\partial DV}\right] \\ &\quad + p[D]\begin{bmatrix} p+\gamma_1 & 0 & 0 \\ 0 & p+\gamma_1 & 0 \\ 0 & 0 & p+\gamma_1 \end{bmatrix}^{-1} \frac{\partial[E]}{\partial DV}\end{aligned} \tag{44}$$

The SVD-based noniterative MIST approximation allows sensitivity calculation [Eq. (42)] without the problems of branch switching and solution jumps or nonconverged iterative MIST results. This makes it possible to compare the sensitivity results of Eq. (43) to those of Eqs. (41) and (42). As numerical tests will show, the difference in the results compared to the full sensitivity analysis (including sensitivities of the singular vectors) is insignificant. Implementation of Eq. (44) to the global case MIST sensitivity with the number of lags greater than one allows us to avoid the convergence and discontinuity problems just discussed and eliminates the need for an iterative process.

D. MIST Sensitivity in the General Case

Based on one-lag term analysis just presented, the sensitivity of the general case can be treated in the similar way. From Eq. (44),

$$\begin{aligned}\left[\frac{\partial Q(p)}{\partial DV}\right] &\approx \left[\frac{\partial A_0}{\partial DV}\right] + p\left[\frac{\partial A_1}{\partial DV}\right] + p^2\left[\frac{\partial A_2}{\partial DV}\right] \\ &\quad + p[D]([I]p - [R])^{-1}\left[\frac{\partial E}{\partial DV}\right]\end{aligned} \tag{45}$$

This is a linear equation for $[\partial A_1/\partial DV]$, $[\partial A_2/\partial DV]$, and $[\partial E/\partial DV]$ [the derivative of the matrix $[A_0]$ is given by Eq. (33)]. Equation (45) is now solved by a single least-squares step without iterations to match:

$$jk_1\left[\frac{\partial A_1}{\partial DV}\right]-k_1^2\left[\frac{\partial A_2}{\partial DV}\right]+jk_1[D]([I]jk_1-[R])^{-1}\left[\frac{\partial E}{\partial DV}\right]\approx\left[\frac{\partial Q(jk_1)}{\partial DV}\right]-\left[\frac{\partial A_0}{\partial DV}\right]$$

$$jk_2\left[\frac{\partial A_1}{\partial DV}\right]-k_2^2\left[\frac{\partial A_2}{\partial DV}\right]+jk_2[D]([I]jk_2-[R])^{-1}\left[\frac{\partial E}{\partial DV}\right]\approx\left[\frac{\partial Q(jk_2)}{\partial DV}\right]-\left[\frac{\partial A_0}{\partial DV}\right]$$

$$\vdots \tag{46}$$

with $[D]$ fixed.

In the following test cases structural sensitivity matrices were obtained by NASTRAN,[19] and frequency-dependent $[Q(jk)]$ matrix sensitivities by the unsteady aerodynamic capability ZAERO.[7,20] Analytic sensitivities, as just described, were used for the MIST approximation terms, while finite difference sensitivities were used in both structural and pure aerodynamic ZAERO matrices. Analytic sensitivities of mass, stiffness, and aerodynamic matrices in the frequency domain can also be obtained analytically using proven aerodynamic and structures sensitivity technology, and the methods of Refs. 7, 15, and 16.

Finally, the MIST approximants at new design points are evaluated based on direct Taylor series created at a reference design point as follows:

$$[A_0]=[A_0]_{\mathrm{REF}}+\left.\frac{\partial[A_0]}{\partial DV}\right|_{\mathrm{REF}}(DV-DV_{\mathrm{REF}}) \tag{47}$$

$$[A_1]=[A_1]_{\mathrm{REF}}+\left.\frac{\partial[A_1]}{\partial DV}\right|_{\mathrm{REF}}(DV-DV_{\mathrm{REF}}) \tag{48}$$

$$[A_2]=[A_2]_{\mathrm{REF}}+\left.\frac{\partial[A_2]}{\partial DV}\right|_{\mathrm{REF}}(DV-DV_{\mathrm{REF}}) \tag{49}$$

$$[E]=[E]_{\mathrm{REF}}+\left.\frac{\partial[E]}{\partial DV}\right|_{\mathrm{REF}}(DV-DV_{\mathrm{REF}}) \tag{50}$$

while the $[D]$ matrix is held frozen, so that $[D]=[D]_{\mathrm{REF}}$.

III. M-W Wing Example

The double-swept forward wing[21] was chosen as an example for the examination of the results of MIST analysis and its sensitivity in the case of major planform changes. The geometry of the wing is shown in Fig. 1, where $c=76$ mm is the chord length, $L=305$ mm is the half-span length, and Λ_i is the sweep angle of the inboard wing, which is varied from -30 to 30 deg. The wing is assumed to have a width $t=1$ mm, and its structural material characteristics are $E=73.8$ GPa, $G=27.6$ GPa, and $\rho=2768$ kg/m^3.

The structural finite element results for the wing for the different values of the inboard sweep angle Λ_i were calculated using MSC NASTRAN (Ref. 19). The first 10 modes were taken for the aeroelastic analysis using Mach $=0$ aerodynamics produced by the ZAERO code (Ref. 20) and a five-lag term MIST rational function approximation. Results of the MIST and the Roger-based state-space models are compared to frequency-domain results using the g method in ZAERO for validation. The MIST process involves the nonlinear double least-squares iteration process.

The divergence and the flutter velocities for different sweep angles are presented in Figs. 2 and 3, respectively. Both velocities increase with the increase of the sweep angle. However the change in divergence velocity is more significant in the case of the swept-backward inner wing, while the change in the flutter velocity is almost monotonic. The divergence velocity, which in the case of the swept-forward wings (in general) is lower than the flutter velocity, is not influenced by the number of MIST lags because it is determined by steady aerodynamics, which is matched exactly.

The choice of five-lag terms MIST approximation (as presented in Fig. 3) was made based on the absolute error [Eq. (30)] of the double least-squares iterative MIST process criteria.

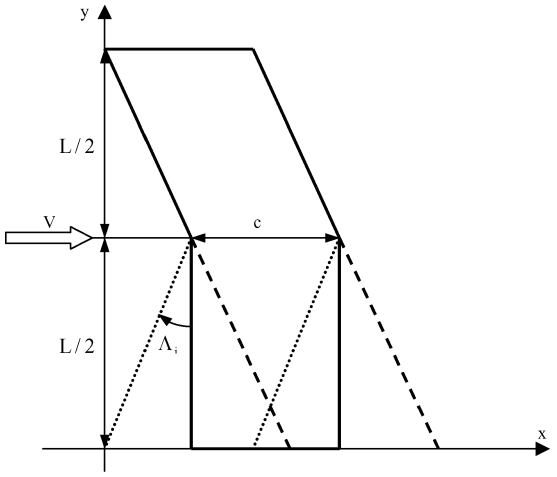

Fig. 1 M-W wing.[21] Planform shape variations of the inner wing are shown.

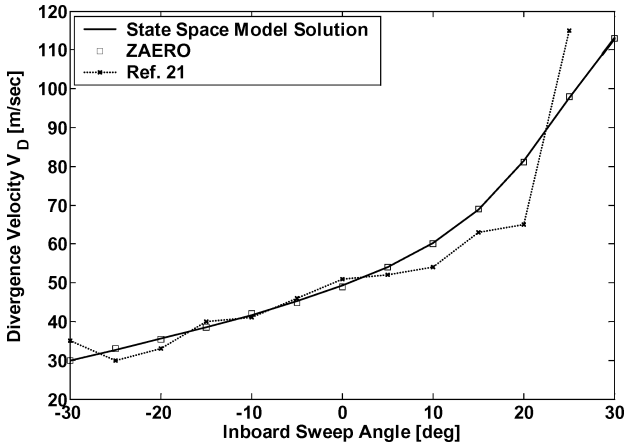

Fig. 2 Divergence speed of the M-W wing as a function of sweep angle of the inner wing.

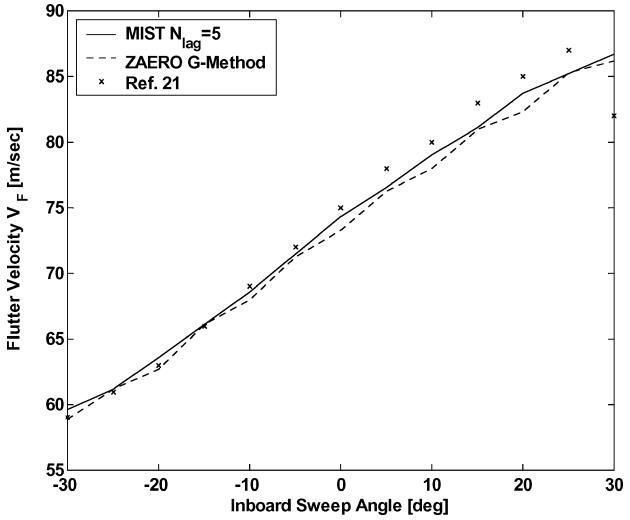

Fig. 3 Flutter speed of the M-W wing as a function of sweep angle of the inner wing.

Table 1 Flutter results obtained by Roger and MIST approximations[a] with different numbers of lag terms[b]

Variable	1	2	3	4	5	6
		Roger				
V_F, m/s	68.9	72.8	74.2	74.3	74.1	74.2
ε [Eq. (30)]	27.6	7.1	2	1.3	0.76	0.51
Total number of states	30	40	50	60	70	80
		MIST				
V_F, m/s	68.9	72.4	74.5	74.5	74.3	74.2
ε [Eq. (30)]	28.9	11.3	5.4	5.2	4.1	3.6
Total number of states	21	22	23	24	25	26

[a]The MIST approximation is generated by the conventional double least-squares iterative process.
[b]The divergence velocity $V_D = 49.2$ m/s.

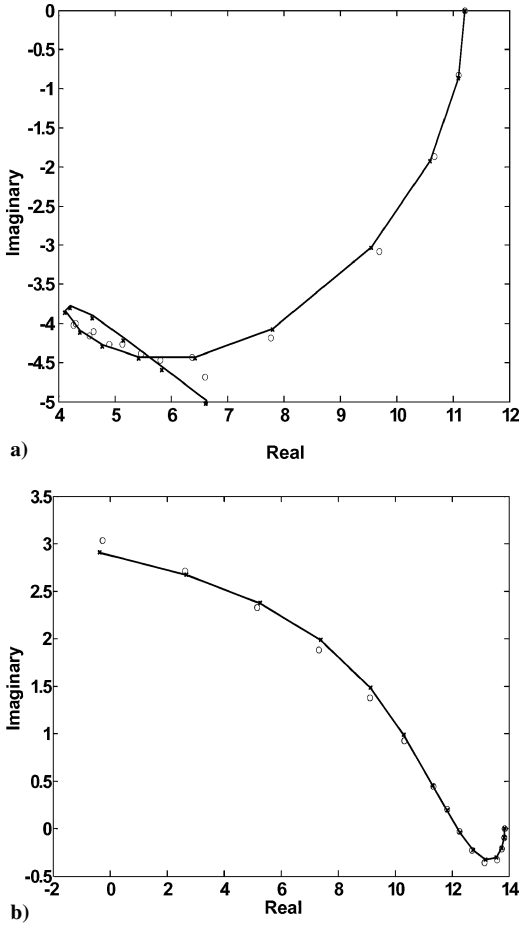

Fig. 4 Quality of MIST approximation with five-lag terms (zero inboard sweep angle case): a) matching the $Q_{53}(k)$ term and b) matching the $Q_{76}(k)$ term.

Table 1 shows results obtained with state-space models based on Roger and MIST approximations. The absolute error for the five-lag term MIST approximation (which adds only five additional aerodynamic states) is relatively small, and one can see a good match in the case of two typical aerodynamic terms: $Q_{5,3}$ and $Q_{7,6}$ (Figs. 4a and 4b).

In both Roger and MIST cases the values of the matching errors decrease when the number of the lags becomes larger. As expected, the decrease in errors of the Roger approximation is more rapid compared to the MIST, although the results for the flutter velocity are similar for the both methods and only slightly changed for $n_{\text{lag}} > 2$.

For the sensitivity analysis the derivatives of the structural and aerodynamic matrices were obtained by finite differences method, as already mentioned. For this purpose the zero inboard sweep angle wing ($\Lambda_i = 0$) was chosen as a reference point, and a new perturbed

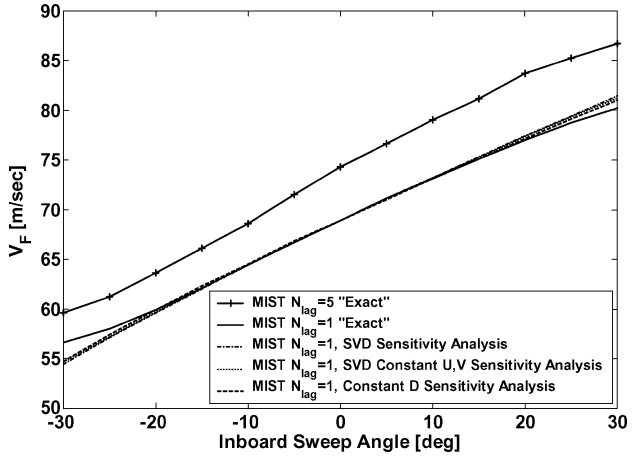

Fig. 5 Flutter speed comparison of the M-W wing as a function of inboard sweep angle based on various sensitivity methods.

model for a forward-Euler finite difference derivative was created at $\Lambda_i = 0.3$ deg.

Figure 5 presents flutter speed results generated to assess performance of the one-lag MIST approximation relative to the more accurate five-lag model. As the figure shows, flutter velocity approximated using only one-lag MIST is up to 8% lower compared to the results with five-lag term approximation, when both MIST approximations were obtained using the conventional double least-squares iterative process. Also shown in the same figure is the one-lag case flutter predictions based on linear extrapolation of aerodynamic matrices from the base design: 1) sensitivity analysis based on SVD approximation of a Roger one-lag model, taking into account sensitivities of both singular values and singular vectors [Eqs. (41) and (42)]; 2) sensitivity based on SVD of the one-lag Roger lag matrix neglecting the sensitivities of the singular vectors [Eq. (43)]; and 3) finally sensitivity analysis based on the solution of a linear set of equations [Eq. (45)], where the $[D]$ matrix is held frozen. One can see a very good agreement between the results of the different approaches, which supports the approach where the MIST matrix derivatives can be efficiently evaluated without an iterative process.

Once the system's matrix $[A]$ is approximated away from the reference design point using direct Taylor series, approximate eigenvalues (for stability analysis of the aeroelastic system) can be generated in two ways: a direct eigenvalues sensitivity method, which is based on the direct approximation of the poles:

$$\lambda_i = \lambda_{i\text{REF}} + \left.\frac{\partial \lambda_i}{\partial DV}\right|_{\text{REF}} (DV - DV_{\text{REF}}) \tag{51}$$

with the analytic sensitivity of eigenvalues given at the reference point by

$$\frac{\partial \lambda_i}{\partial DV} = \frac{\{L_{\text{vec}_i}\}^*(\partial[A]/\partial DV)\{R_{\text{vec}_i}\}}{\{R_{\text{vec}_i}\}^*\{L_{\text{vec}_i}\}} \tag{52}$$

where $\{L_{\text{vec}_i}\}$ and $\{R_{\text{vec}_i}\}$ are the left and right eigenvectors of the matrix $[A]$, respectively. A reciprocal Taylor-series or a Rayleigh quotient approximation can also be used.[15]

Alternatively, the direct state-space model sensitivity analysis can be used: the $[A]$ matrix is approximated using direct and reciprocal Taylor series:

$$[A] = [A]_{\text{REF}} + \left.\frac{\partial [A]}{\partial DV}\right|_{\text{REF}} (DV - DV_{\text{REF}}) \tag{53}$$

and a full eigenvalue analysis is carried out for the aeroelastic poles.

This process separates the generation of approximated $[A_0]$, $[A_1]$, $[A_2]$, [D], [E] matrices (which in our case are created using Taylor-series extrapolation from the reference configuration) and the generation of aeroelastic poles for an approximated $[A]$ matrix (which

can be done by full eigenvalue solution or by Taylor series or RQA approximations of the eigenvalues).

Figure 6 shows the behavior of the real and the imaginary parts of the flutter eigenvalue with respect to the flight velocity in a case of $\Lambda_i = -5$ deg. The method based on the full eigenvalue analysis is more costly in terms of the calculation time. Its results, however, show better match (to the results of full new aerodynamic, structural, and aeroelastic analysis at new design points) compared to the results of the Taylor series for the poles based on direct eigenvalues sensitivities [Eq. (51)].

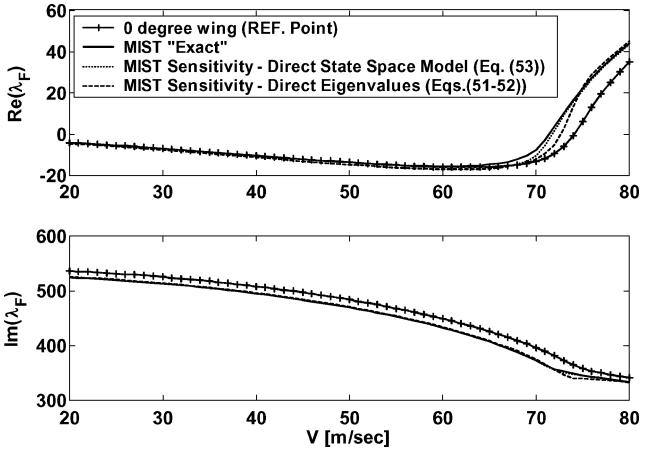

Fig. 6 Behavior of flutter eigenvalue for different methods vs flight velocity. The inboard sweep angle is −5 deg with five-lag MIST approximation.

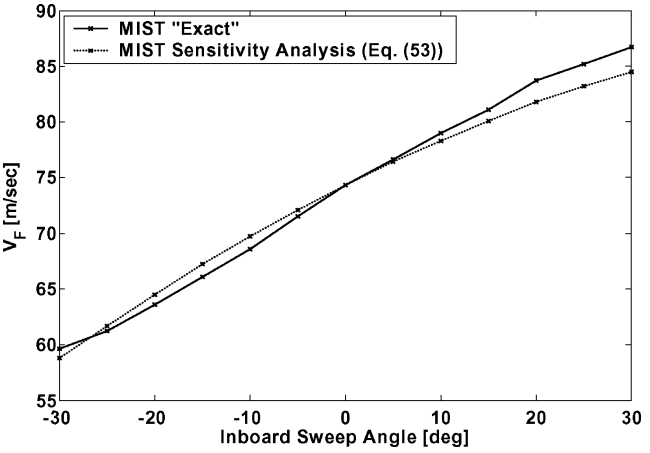

Fig. 7 Flutter speed of the M-W wing as a function of inboard sweep angle. MIST approximations: full eigenvalue analysis with Taylor-series-based $|A|$ matrix in a case of five-lag terms MIST approximation.

It is preferable to use Eqs. (51) and (52) in the cases where the absolute value of the inboard sweep angle is within the range of 5 deg (or up to 15% change from the initial design point). Full eigenvalue analysis with an approximated system matrix [Eq. (53)] shows better results when the shape variation away from the reference design is larger.

Figure 7 shows the flutter speed vs the inboard sweep angle of the wing. Mathematically, the flutter occurs when the real part of one of the system's eigenvalues (which, in the case of Fig. 7, were calculated based on the full eigenvalue analysis with an approximated $[A]$ matrix) becomes positive. The flutter results show very good agreement in the entire range of the inboard sweep angle -30 deg $\leq \Lambda_i \leq 30$ deg, keeping the error less than 3%.

Despite the fact that the flutter velocity is well approximated in the entire range of Λ_i by the first-order Taylor-series approximation of the system's matrix $[A]$ at the reference point $\Lambda_i = 0$, the differences in the system's behavior (compared to "exact" analysis of the system at the new design point) become considerable for $|\Lambda_i| > 15$ deg. This is shown in Figs. 8a and 8b, which present enlarged part of root locus plots for 15 and 30 deg of the inboard sweep angle. For 15 deg the eigenvalues of the sensitivity analysis are in the range of a few percent of the error. However, in the case of 30 deg of the inboard sweep angle, the error is much higher; therefore, a new initial point has to be chosen, and the new derivatives in this point should be evaluated.

IV. Conclusions

A method for obtaining sensitivities of unsteady aerodynamic minimum-state (MIST) approximation matrices with respect to planform shape design variables of general flight vehicle configurations was presented in this paper. The commonly used minimum-state approximation generation process is iterative and subject to discontinuous behavior of the resulting matrices. The paper identified a particular case in which minimum-state approximations can be found using singular value decomposition of a Roger lag matrix without any iteration. By using this case, insights were developed regarding alternative MIST sensitivity equations, and a preferred method was suggested for calculating MIST sensitivities that are not subject to convergence and discontinuity problems. Approximations of flutter speeds and aeroelastic poles based on the shape sensitivity of the system's aeroelastic state-space matrix were compared to exact results for a M-W wing subject to considerable sweep variation of its inboard section. MIST approximants created by Taylor-series extrapolation of MIST matrices, based on aerodynamic, structural, and MIST analysis and sensitivity analysis at a reference design shape, performed well over quite a wide range of shape variation of the M-W wing. Extension of MIST shape sensitivities and approximations of aeroservoelastic model variation (with respect to shape changes) to cases of gust response and active aeroelastic control is currently under study.

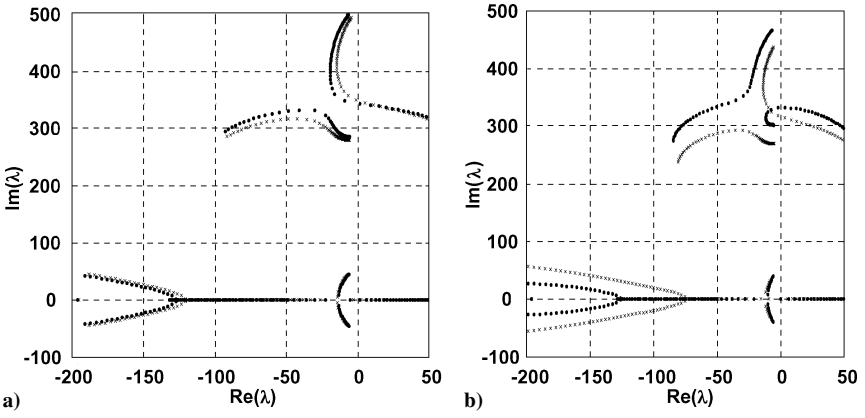

Fig. 8 Part of root locus of the M-W wing with an inboard sweep angle of Λ_i = a) −15 and b) −30 deg: exact results vs full eigenvalue analysis with Taylor-series-based $|A|$ matrix.

Appendix: One-Aerodynamic-Lag-Term MIST–Roger Approximation Relation

For a square, nonsingular matrix $[A]$ the singular value decomposition can be presented as follows:

$$[A]_{n\times n} = [U]_{n\times n}[V]_{n\times n} = \{U_1\}_{n\times 1}\{V^1\}_{1\times n} + \{U_2\}\{V^2\} + \cdots + \{U_n\}\{V^n\} = \sum_{i=1}^{n}\{U_i\}_{n\times 1}\{V^i\}_{1\times n} \quad \text{(A1)}$$

where $\{U_i\}$ are columns of the $[U]$ matrix (subscripts denote columns) and $\{V^i\}$ are rows of the $[V]$ matrix (superscripts denote rows). The matrices $[U]$ and $[V]$ contain the left and right singular vectors of the matrix $[A]$, respectively. They are normalized to satisfy

$$[U]^T[U] = [S]^2 \quad \text{(A2)}$$

$$[V][V]^T = [I] \quad \text{(A3)}$$

Here $[S]$ is the diagonal matrix of the singular values.

Let the double least-squares process of the MIST procedure be used to approximate a given matrix $[A]$ using a single left column vector $\{\bar{D}_1\}$ and a single right row vector $\{\bar{E}^1\}$:

$$\{\bar{D}_1\}_{n\times 1}\{\bar{E}^1\}_{1\times n} \approx [A]_{n\times n} \quad \text{(A4)}$$

The column vector $\{\bar{D}_1\}$ and row vector $\{\bar{E}^1\}$ can be presented as a linear combination of the columns of $[U]$ and the rows of $[V]$ as follows:

$$\{\bar{D}_1\} = \alpha_1\{U_1\} + \alpha_2\{U_2\} + \cdots + \alpha_n\{U_n\} = \sum_{i=1}^{n}\alpha_i\{U_i\} \quad \text{(A5)}$$

$$\{\bar{E}^1\} = \beta_1\{V^1\} + \beta_2\{V^2\} + \cdots + \beta_n\{V^n\} = \sum_{i=1}^{n}\beta_i\{V^i\} \quad \text{(A6)}$$

Following the MIST double least-squares process, the vector $\{\bar{D}_1\}$ is frozen at some initial guess, and a least-squares solution for the $\{\bar{E}^1\}$ is sought:

$$\{\bar{E}^2\}_{1\times n} = (\{\bar{D}_1\}^T\{\bar{D}_1\})^{-1}\{\bar{D}_1\}^T[A] \quad \text{(A7)}$$

Using the orthogonality property of the singular vectors ($\{U_i\}^T\{U_j\} = 0,\ i \neq j$ [Eq. (A2)], one obtains

$$\{\bar{D}_1\}^T\{\bar{D}_1\} = \sum_{i=1}^{n}\left(\alpha_i\{U_i\}^T\right)\cdot\sum_{j=1}^{n}(\alpha_j\{U_j\}) = \sum_{i=1}^{n}(s_i\alpha_i)^2 \quad \text{(A8)}$$

also,

$$\{\bar{D}_1\}^T[A] = \sum_{i=1}^{n}\alpha_i\{U_i\}^T\cdot\sum_{j=1}^{n}\{U_j\}\{V^j\} = \sum_{i=1}^{n}\alpha_i s_i^2\{V^i\} \quad \text{(A9)}$$

Substituting Eqs. (A8) and (A9) into Eq. (A7) gives

$$\{\bar{E}^1\}_{1\times n} = \frac{\sum_{i=1}^{n}\alpha_i s_i^2\{V^i\}}{\sum_{i=1}^{n}(s_i\alpha_i)^2} \quad \text{(A10)}$$

Using the expression for $\{\bar{E}_1\}$ from Eq. (A6) with Eq. (A10), based on linear combination properties, one finds

$$\beta_i = \frac{\alpha_i s_i^2}{\sum_{j=1}^{n}(s_j\alpha_j)^2} \quad \text{(A11)}$$

The next stage of the double least-squares process is to freeze $\{\bar{E}_1\}$ and solve in a least-squares manner for a new $\{\bar{\bar{D}}_1\}$. However, back to Eq. (A4), the solution for the column vector $\{\bar{D}_1\}$ is

$$\{\bar{\bar{D}}_1\}_{n\times 1} = [A]\{\bar{E}^1\}^T(\{\bar{E}^1\}\{\bar{E}^1\}^T)^{-1} \quad \text{(A12)}$$

The new vector can be expressed as [Eq. (A5)]

$$\{\bar{\bar{D}}_1\} = \bar{\alpha}_1\{U_1\} + \bar{\alpha}_2\{U_2\} + \cdots + \bar{\alpha}_n\{U_n\} = \sum_{i=1}^{n}\bar{\alpha}_i\{U_i\} \quad \text{(A13)}$$

with $\bar{\alpha}_1$ being new coefficients. Using Eq. (A6),

$$\{\bar{E}^1\}\{\bar{E}^1\}^T = \sum_{i=1}^{n}\beta_i\{V^i\}\sum_{j=1}^{n}\beta_j\{V^j\}^T = \sum_{i=1}^{n}\beta_i^2 \quad \text{(A14)}$$

$$[A]\{\bar{E}^1\}^T = \sum_{i=1}^{n}\{U_i\}\{V^j\}\sum_{j=1}^{n}\beta_j\{V^j\}^T = \sum_{i=1}^{n}\beta_j\{U_i\} \quad \text{(A15)}$$

Clearly, from Eqs. (A11–A15)

$$\bar{\alpha}_i = \frac{\beta_i}{\sum_{k=1}^{n}\beta_k^2} \quad \text{(A16)}$$

Using Eq. (A11), one can relate the new values of $\bar{\alpha}_i$ to the values from the previous iteration α_k

$$\left(\sum_{k=1}^{n}\beta_k^2\right)\bar{\alpha}_i = \beta_i = \frac{\alpha_i s_i^2}{\sum_{j=1}^{n}(s_j\alpha_j)^2} \quad \text{(A17)}$$

Now

$$\sum_{k=1}^{n}\beta_k^2 = \sum_{k=1}^{n}\left[\frac{\alpha_k s_k^2}{\sum_{j=1}^{n}(s_j\alpha_j)^2}\right]^2 = \frac{\sum_{k=1}^{n}\left(\alpha_k s_k^2\right)^2}{\left[\sum_{j=1}^{n}(s_j\alpha_j)^2\right]^2} \quad \text{(A18)}$$

Eliminating the β terms completely from Eq. (A17), the following expression is obtained:

$$\frac{\sum_{k=1}^{n}\left(\alpha_k s_k^2\right)^2}{\left[\sum_{j=1}^{n}(s_j\alpha_j)^2\right]^2}\bar{\alpha}_i = \frac{\alpha_i s_i^2}{\sum_{j=1}^{n}(s_j\alpha_j)^2} \quad \text{(A19)}$$

Finally,

$$\bar{\alpha}_i = \frac{\sum_{j=1}^{n}(s_j\alpha_j)^2}{\sum_{k=1}^{n}\left(\alpha_k s_k^2\right)^2}\alpha_i s_i^2 \quad \text{(A20)}$$

Suppose that one starts the double least-squares process with $\{\bar{D}_1\} = \{U_1\}$, then $\alpha_1 = 1, \alpha_2 = 0, \alpha_3 = 0$, and .... In this case Eq. (A20) leads to $\bar{\alpha}_1 = \alpha_1, \bar{\alpha}_2 = 0, \bar{\alpha}_3 = 0$, and .... The new $\{\bar{\bar{D}}_1\}$ vector is identical to $\{\bar{D}_1\}$ vector from the preceding iteration, and the process is converged. That is, starting with *any* left singular vector as the initial guess for $\{D\}$, the MIST iteration will converge to the same vector after a single $\{\bar{D}\} \rightarrow \{\bar{E}\} \rightarrow \{\bar{D}\}$ iteration. Selection of singular vectors of a square $[A]$ as initial guesses for the MIST approximation makes the MIST iteration unnecessary. The advantage, in addition to the elimination of the iterative process, is that with singular vectors and singular values in the $[D][E]$ approximation of $[A]$, sensitivities of $[D]$ and $[E]$ are well defined once the sensitivity of $[A]$, $\partial[A]/\partial DV$, is given.

Acknowledgments

Support by NASA (Peter Coen, Grant Monitor) is gratefully acknowledged.

References

[1]Livne, E., "Integrated Aeroservoelastic Optimization: Status and Progress," *Journal of Aircraft*, Vol. 36, No. 1, 1999, pp. 122–145.

[2]Yates, E. C., Jr., "Aerodynamic Sensitivities from Subsonic, Sonic, and Supersonic Unsteady, Nonplanar Lifting Surface Theory," NASA TM 100502, Sept. 1987.

[3]Yates, E. C., Jr., "Integral Equation Methods in Steady and Unsteady Subsonic, Transonic, and Supersonic Aerodynamics for Interdisciplinary Design," NASA TM 102677, May 1990.

[4]Livne, E., and Li, W.-L., "Aeroservoelastic Poles: Their Analytic Sensitivity and Alternative Approximations in Wing Planform Shape Synthesis," *Aeroelasticity and Fluid Structure Interaction Problems*, AD-Vol. 44, edited by P. P. Friedmann and J. C. I. Chang, American Society of Mechanical Engineers, 1995, pp. 99–123.

[5]Livne, E., and Li, W.-L., "Aeroservoelastic Aspects of Wing/Control Surface Planform Shape Optimization," *AIAA Journal*, Vol. 33, No. 2, 1995, pp. 302–311.

[6]Li, W.-L., and Livne, E., "Analytic Sensitivities and Approximations in Supersonic and Subsonic Wing/Control Surface Unsteady Aerodynamics," *Journal of Aircraft*, Vol. 34, No. 3, 1997, pp. 370–379.

[7]Chen, P. C., Liu, D. D., and Livne, E., "Unsteady Aerodynamic Shape Sensitivities for Airplane Aeroservoelastic Configuration Optimization," AIAA Paper 2004-1759, April 2004.

[8]Karpel, M., "Size Reduction Techniques for the Determination of Efficient Aeroservoelastic Models," *Control and Dynamic Systems—Advances in Theory and Applications*, Vol. 54, Academic Press, 1992, pp. 263–295.

[9]Roger, K. L., "Airplane Math Modeling Methods for Active Control Design," *Structural Aspects of Active Controls*, AGARD, 1977, pp. 4–11.

[10]Karpel, M., "Design for Active Flutter Suppression and Gust Alleviation Using State Space Aeroelastic Modeling," *Journal of Aircraft*, Vol. 19, No. 3, 1982, pp. 221–227.

[11]Tiffany, S. H., and Adams, W. M., "Nonlinear Programming Extensions to Rational Function Approximations of Unsteady Aerodynamic Forces," NASA TP 2776, 1988; also AIAA Paper 87-0854, 1987.

[12]Karpel, M., "Time-Domain Aeroservoelastic Modeling Using Weighted Unsteady Aerodynamic Forces," *Journal of Guidance, Control, and Dynamics*, Vol. 13, No. 1, 1990, pp. 30–37.

[13]Karpel, M., and Strul, E., "Minimum-State Unsteady Aerodynamic Approximations with Flexible Constraints," *Journal of Aircraft*, Vol. 33, No. 6, 1996, pp. 1190–1196.

[14]Karpel, M., "Reduced-Order Models for Integrated Aeroservoelastic Optimization," *Journal of Aircraft*, Vol. 36, No. 1, 1999, pp. 146–155.

[15]Haftka, R. T., and Gurdal, Z., *Elements of Structural Optimization*, 3rd ed., Kluwer Academic, 1992.

[16]Kamat, M. P., *Structural Optimization: Status and Promise*, Vol. 150, Progress in Astronautics and Aeronautics, AIAA, Washington, DC, 1993.

[17]Haftka, R. T., "Sensitivity Calculations for Iteratively Solved Problems," *International Journal for Numerical Methods in Engineering*, Vol. 21, 1985, pp. 1535–1546.

[18]Newsom, J. R., and Mukhopadhyay, V., "A Multiloop Robust Controller Design Study Using Singular Value Gradients," *Journal of Guidance, Control, and Dynamics*, Vol. 8, No. 4, 1985, pp. 514–519.

[19]Schaeffer, H. G., *MSC.NASTRAN Primer for Linear Analysis*, 2nd ed., MSC Software, Santa Ana, CA, 2001.

[20]Yurkovich, R., "Status of Unsteady Aerodynamic Prediction for Flutter of High Performance Aircraft," *Journal of Aircraft*, Vol. 40, No. 5, 2003, pp. 832–842.

[21]Koo, K. N., "Aeroelastic Characteristics of Double-Swept Isotropic and Composite Wings," *Journal of Aircraft*, Vol. 38, No. 2, 2001, pp. 343–348.

S. Saigal
Associate Editor